ARTICLE

Check for updates

Spatial gradients of urban land density and nighttime light intensity in 30 global megacities

Muchen Zheng [1,3], Wenli Huang [1,3], Gang Xu [1✉], Xi Li[2] & Limin Jiao[1]

The spatial agglomeration of urban elements results in the center-periphery urban structure, but the difference in spatial gradients of socioeconomic and physical elements is unclear. This study investigates how urban land density (ULD) and nighttime light intensity (NLI) decline with the distance to center(s) using the inverse-S function. Taking 30 global megacities as examples, we acquired their urban land and nighttime light in 2020 to represent urban physical and socioeconomic elements, respectively. ULD and NLI in concentric rings have been calculated to compare their spatial gradients from the city center(s). Results show that both ULD and NLI decrease slowly around city centers, followed by a relatively quick decline to suburban areas, and then decrease slowly again to a background level, showing an inverse-S shape. This spatial gradient can be well-fitted by the inverse-S function, whose parameters reflect disparities in urban extents and urban forms. NLI decreases faster than ULD, resulting in smaller radii (extents) of NLI, which shows the spatial agglomeration of socioeconomic elements is more obvious than that of physical space. This gap requires balanced development of socioeconomic and physical elements in megacities to avoid low-density urban sprawl and promote sustainable urban development.

[1] School of Resource and Environmental Sciences, Wuhan University, 430079 Wuhan, China. [2] State Key Laboratory of Information Engineering in Surveying, Mapping and Remote Sensing, Wuhan University, 430079 Wuhan, China. [3] These authors contributed equally: Muchen Zheng, Wenli Huang. ✉email: xugang@whu.edu.cn

Introduction

More than half of the world's population is now residing in cities, and this proportion is continuing to increase in the near future (Angel, 2012). Urbanization is a crucial social transformation across the world in this century, closely related to our environment, climate, and global sustainability (Duarte, Álvarez, 2019; Seto et al., 2010). Monitoring urban land-cover changes and characterizing urban expansion is a common concern shared by environmentalists, urban planners, geographers, and other scientists (Reba, Seto, 2020; Xu et al., 2019).

Spatial agglomeration is an essential feature that distinguishes the city from the countryside (Scott, Storper, 2015). Despite the constant outward expansion of cities, industrial and economic activities in cities are excessively concentrated in places with abundant resources, convenient transportation, and favorable locations (Geddes, 1915). These places are most likely to be the centers of urban development. Central Place Theory explains the hierarchical organization of cities (Christaller, 1966). The city center serves as a core area with concentrated functions such as commerce, politics, culture, and transportation (Harris, Ullman, 1945). Urban population is mainly concentrated in the core areas, resulting in positive feedback leading to the agglomeration of other elements. Thus, the urban population gradually declines with the distance from the city centers and various urban elements also show a similar spatial agglomeration and gradient (Li et al., 2021). In the process of urban expansion from the center to the periphery, there exist concentric zones with unique social and economic characteristics according to concentric zone theory (Burgess, 2008). Concentric partitioning has been commonly used to measure urban elements from the city center outward quantitively (Seto, Fragkias, 2005; Taubenböck et al., 2009).

The process of urban growth is different in physical and social spaces, especially in megacities. The impervious surface acquired from remotely sensed data is the direct representation of urban expansion (Patino, Duque, 2013; Van de Voorde et al., 2011), but it neglects the urban dynamics of socioeconomic activities. The nighttime light satellite imagery can inspect the intensity and spatial disparity of urban dynamics (Bagan, Yamagata, 2015; Li, et al., 2015), which has been successfully applied to monitor and characterize urban growth, detect socioeconomic dynamics, and estimate energy consumption (Bennett, Smith, 2017; Letu et al., 2010; Levin et al., 2020). As an appropriate proxy to measure the intensity of socioeconomic activities, nighttime light is a comprehensive indicator that conveys information from spatial distribution, economy, and other factors influencing urban development (Bennett, Smith, 2017; Mård et al., 2018). Nighttime light shows a solid ability to assess urban development in terms of both spatial and socioeconomic status (Elvidge et al., 2023) and can provide insights into the identification of urban structure and the state of urban development (Kyba et al., 2017; McCallum et al., 2022; Ren et al., 2022). The Visible Infrared Imaging Radiometer Suite (VIIRS) nighttime light imagery acquired by the Suomi National Polar-orbiting Partnership (NPP) Satellite is widely used for regional economy and urban studies because of its high spatial resolution and high sensitivity of visible light (Li et al., 2022b).

The difference between socioeconomic activities and land use development in cities is often caused by excessive urban sprawl (Xu et al., 2022; Yasi et al., 2020). The rapid expansion of urban land resulted in an increase in land take per person across the globe in recent decades (Li et al., 2022a). Previous studies on the spatial distribution of urban elements mainly focus on population and urban land (Akbar et al., 2019; Batty, Sik Kim, 1992; Kroll, Haase, 2010; Song, Yu, 2019). In terms of quantitative models describing urban land density spatial patterns, previous studies proposed a linear model with two stages, inverse-S function, and

Geographic Micro-Process (GMP) models to describe the spatial distribution of urban land (Guérois, Pumain, 2008; Jiao, 2015; Jiao et al., 2021). The spatial distribution of other elements except urban land also plays a key role in the analysis of urban expansion (Cai et al., 2021; Chen et al., 2022, Yang et al., 2023). The spatial distribution of different urban elements determines the internal structure of each city, and the mismatch between them hinders the sustainable development of cities (Xiao et al., 2021).

The growth of cities is uneven among different-sized cities (Shukla et al., 2021). More and more people transfer to large cities, making large cities grow into megacities with more than ten million residents (Huang et al., 2017). For example, the total urban population in developed countries has not increased in recent decades, but their large cities have been expanding and growing (Zhang, 2016). The world's largest urbanized region, Tokyo, Japan, has accommodated more than 35 million urban residents (Bagan, Yamagata, 2012). Studying the urban expansion and urban spatial structure of megacities has a positive significance for guiding urban development, especially for the development of small and medium-sized cities (Novotný et al., 2022).

In this study, we first choose 30 megacities with prominent political and economic status across the world as sample cities. We use the land use/cover data to reflect the physical expansion of cities and nighttime light to represent the intensity of urban dynamics in social space. We analyze the spatial gradients of nighttime light and urban land density to fully quantify the pattern and dynamics of urban expansion in megacities and provide policy implications for global sustainable development.

Study area and data

Study area. We selected 30 cities around the world, including 21 megacities with a population of more than 10 million and 9 regional central cities with prominent political and economic status, such as Berlin, Rome, Madrid, and so on. Population is not the only criterion for selection because most cities with huge populations are located in East Asia, while some essential European and African cities have relatively small populations due to the constraints of terrain, economy, and other conditions. Therefore, to ensure the representativeness of sample cities on a global scale, we select 30 cities that can reflect the current urban physical and social spatial relationships around the world. With the rapid urban expansion in the past few decades, these megacities are the central cities of various countries, which can provide a reliable theoretical basis for the comparison of global urban expansion (Fig. 1).

Data and pre-processing. Land use and nighttime light data were used to compare the differences between physical and social expansions of cities. We used land use data in 2020 derived from the ESRI 10 m Global Land Cover products (https://livingatlas.arcgis.com/landcover/), which is mapped based on Sentinel-2 scene collection. The production provides a 9-class map of the surface, including vegetation types, bare surface, water, cultivated land, trees, grass, scrub, built-up areas, and snow/ice. As water bodies are deemed incapable of conversion to urban land, the land use products were reclassified into three types: built-up areas, water bodies, and open space. Open space covers other types of land, which may have the potential to be converted into urban land. The yearly composite of NPP-VIIRS nighttime light of 2020 was applicated to characterize the urban forms in social space (https://eogdata.mines.edu/nighttime_light/annual/v20/). Administrative boundaries data was used to clip the images and extract the selected study area of the 30 megacities, which are

from the Database of Global Administrative Areas (https://gadm.org/).

Methods

Concentric ring analysis. Concentric ring analysis is used to explore the spatial pattern of urban elements. A series of equidistant concentric rings are built outward from the centers of the cities (Schneider, Woodcock, 2008). A buffer ring is a basic unit for calculating urban land density and nighttime light intensity. The scale effects caused by the differences in the resolution of land use and nighttime light data can be eliminated after calculation. Using Google high-resolution imagery, we define the central business district (CBD) or the birthplace of a city as its city center (Burgess, 2008; Jiao, 2015; Yu et al., 2021). The spatial extents of urban land in 2020 determine urban boundaries. And the extent of the series of equidistant buffer rings should ensure that the buffers cover the main area of the cities. Taking Beijing (China) as an example, the concentric rings are shown in Fig. 2a.

Urban land density is defined as the proportion of built-up areas to buildable areas in a buffer ring (Jiao, 2015; Xu et al., 2019). The urban land density of a buffer ring is calculated using formula (1):

$$Dens = \frac{S_{\text{urban land}}}{S - S_{\text{water}}} \quad (1)$$

where $Dens$ is the urban land density of a ring. S is the total land area in a ring. $S_{\text{urban land}}$ and S_{water} are the areas of built-up areas and water bodies in a ring, respectively.
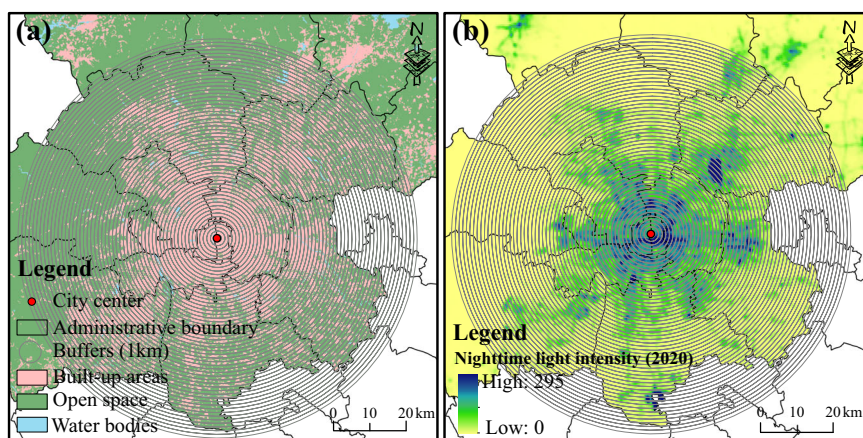
The nighttime light intensity in concentric rings is defined as the ratio of total digital number values of nighttime light to the area of a concentric ring. The nighttime light intensity is standardized, that is, linearly scaled to [0, 1]. The normalization formula of nighttime light data is:

$$DN_i' = \frac{DN_i - DN_{\text{min}}}{DN_{\text{max}} - DN_{\text{min}}} \quad (2)$$

where DN_i' is the mean value of the NLI of the ith ring after standardized treatment, DN_i is the mean value of the NLI of the ith ring from the city center. DN_{min} and DN_{max} are the minimum and maximum value of the NLI of all the rings.

Fig. 1 Spatial distribution of 30 sample cities. (Demographic data is from https://worldpopulationreview.com/).

Fig. 2 Concentric ring analysis using 1-km series buffers in Beijing, China. a Urban land density. **b** Nighttime light intensity. The unit of nighttime light radiance is nW·cm^{-2}·sr^{-1}.

Inverse-S function. The spatial distribution of urban land density presents an inverse-S shape. The density of urban land is the highest in the urban center, and with increasing distance from the city center, it slowly decays in the core areas. Then, it decreases relatively fast in the inner and suburban areas, and finally slowly decays in the periphery of the city. Jiao (2015) proposed a modified function with an inverse-S shape (*inverse-S function*) to characterize the spatial gradients of urban land density. The inverse-S function is defined in formula (3):

$$f(r) = \frac{1-c}{1 + e^{\alpha(\frac{2r}{D}-1)}} + c \qquad (3)$$

where f is the urban elements calculated using formula (1) and formula (2), r is the radius from the city center to a buffer ring, e is Euler's number, and α, c and D are parameters.

The parameters can characterize the urban form. Parameter c represents the background density of urban land or nighttime light in the periphery of a city and parameter D is the city radius. Since parameter α is negatively correlated with the proportion of the rapidly decreasing part of the curve, it is regarded as the representation of the compactness of a city (see detailed explanations in Jiao (2015)).

The urban land density function has been widely used, covering many countries and cities around the world (Keeratikasikorn, 2018; Shukla et al., 2021; Xu et al., 2019). Urban elements generally show the nature of spatial agglomeration and have similar spatial distribution patterns. Thus, in addition to the urban land density, the distribution of other geographical elements also follows an "inverse-S shape rule". Previous studies have applied the urban land density function to population density, road density, and land surface temperature (Bonafoni, Keeratikasikorn 2018; Govind, Ramesh 2020; Li et al., 2021).

Concentration degree index. To compare the spatial agglomeration scope of nighttime light and urban land, we adopted the ratio of parameter D between nighttime light intensity and urban land density, which was named concentration degree index (*CDI*) (Li et al., 2021). *CDI* laterally reflects the relationship between nighttime light intensity and urban land density of each city and builds a bridge between urban social space and physical space. The index can be written as:

$$CDI = \frac{D_{NLI}}{D_{ULD}} \qquad (4)$$

where D_{NLI} and D_{ULD} are fitted parameter D for the nighttime light intensity and urban land density, respectively. For a city with a larger *CDI*, its spatial size in social space is closer to its physical size.

Results
Spatial patterns of urban land and nighttime light. The spatial distribution of urban land and nighttime light of the 30 megacities in 2020 are shown in Figs. 3 and 4, respectively. The diversity of spatial distribution of various elements in cities can be attributed to factors such as geographical location, policy planning, and development direction. Overall, both land use and nighttime light exhibit a circular spatial pattern with a center-periphery structure, indicating a certain degree of similarity. Figure 3 primarily displays the cities' land use, which shows a high density of urban land near the city centers, gradually decreasing towards the cities' periphery due to land expansion. The distribution patterns of nighttime light and urban land are also similar, with higher nighttime light intensity observed in the urban core area and reduced intensity towards the urban edge

area (Fig. 4). However, the main scope of the cities in social space is much smaller than the size of cities in physical space.

Nighttime light helps to identify whether urban land exists and to highlight the intensity of social and economic activities. In recent years, the urban expansion mode of megacities has changed from "extension" to "infill" (Xu et al., 2020). Built-up areas in central areas of cities are contiguous with relatively scattered forms, showing compactness in the images, and boundaries between various areas in cities are not obvious. In contrast, high-intensity patches in nighttime light images are more dispersed and interconnected, but easily distinguishable. Greater socioeconomic activities are more likely to be identified. In addition, Figs. 3 and 4 reveal that although megacities have experienced drastic urban expansion and the urban land density has increased significantly, socioeconomic activities are not active in urban fringe areas because of the higher rate of land expansion than the rate of population growth (Seto et al., 2011).

Spatial gradients of urban land density and nighttime light intensity. Urban land density and nighttime light intensity have been calculated in each concentric ring (Fig. 2). The distance decay of the two elements with the city center is shown in Fig. 5. We use the inverse-S function to fit spatial gradients of the urban land density and nighttime light intensity. The parameters of fitting curves are shown in Table 1. For urban land density, the fitting results show the radius and compactness of cities in physical space. NLI indicates the agglomeration of urban socioeconomic activities and the scale of cities in social space. The fitting curves of the two urban elements in each city both show an obvious inverse-S shape, that is, slow decay around the central areas, then fast decay, and finally slow decay again in the hinterland of the cities. Urban land density in most cities showed a more complete inverse-S shape spatial gradient. However, NLI decays rapidly in the core areas of the cities, and the first slow decay interval is not obvious. The spatial gradient of NLI is more agglomerate. The gap between the fitting curves of the two urban elements is too large at the same distance from the city center. On the one hand, the clustering effect of nighttime light is more obvious, so the intensity attenuation is more rapid. On the other hand, after normalization, NLI at the city edge is close to 0, which is different from the actual density of urban land.

The inverse-S function has good fitting results for both types of urban elements, with R^2 of all cities above 0.85 (Table 1). Parameter α controls the slope of the fitting curve of the inverse-S function, which is related to the compactness of the cities. Larger values of α indicate that the cities are more compact. The values of α of the urban land density are generally larger than that of nighttime light intensity. The values of α fitted by urban land density in sample cities range from 1.54 to 5.92 with an average of 3.49. The parameters α of the nighttime light intensity ranges from 0.68 to 3.73 with an average of 2.04. The constant c is the value of the density of urban elements in the hinterland of the cities, and generally, the value of c is less than 0.3. In some cities such as Shanghai, New York, and Kolkata, as the megacities are expanding to saturation, there is still a large density value on the outskirt of the cities, so the c value fitted by the density of urban land may be rather large. The parameter D represents the radius of the main area of a city. Larger values of D fitted by urban land density indicate larger urban entities. Likewise, a larger value of D of NLI means a larger urban scale in social space, which is consistent with Figs. 2 and 3. The urban radii fitted by the density of built-up areas are generally larger than that of nighttime light intensity.
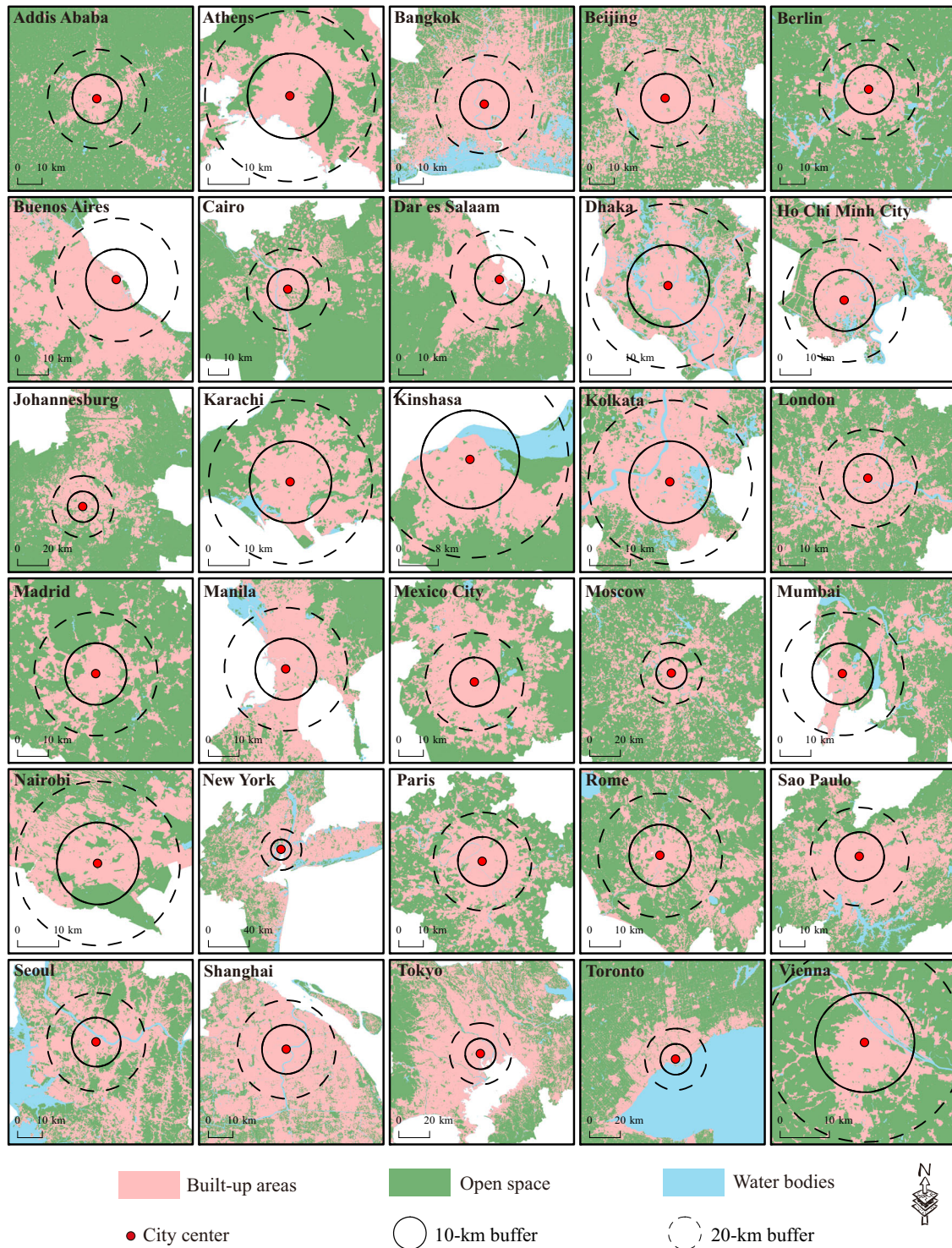
Fig. 3 Urban land use in three types of built-up areas, open space, and water bodies in 30 megacities in 2020. Two buffers with radii of 10 km and 20 km show the extents of sample cities. (Data Source: https://livingatlas.arcgis.com/landcover/).

Comparisons of urban form and urban extent. The comparison of parameters of the inverse-S function between urban land density and nighttime light intensity is shown in Fig. 6. In the case of a compact urban form, the ULD curve is characterized by a higher density in the urban core area that decreases rapidly in the surrounding area, leading to a steep curve (Jiao, 2015; Li et al., 2021). On the contrary, the urban land density curve of the sprawling urban form decreases more slowly. Jiao (2015) defines compactness as the proportion of the rapidly decaying region to the overall part of the curve, which is linearly related to the parameter α that controls the slope of the curve. Therefore, parameter α represents urban compactness, and a larger value of α indicates a more compact urban form. It clearly shows that nighttime light intensity declines more rapidly outward from city centers, which made the fitting curves of NLI exhibit a steeper slope but also a longer interval of rapid decay. The socioeconomic
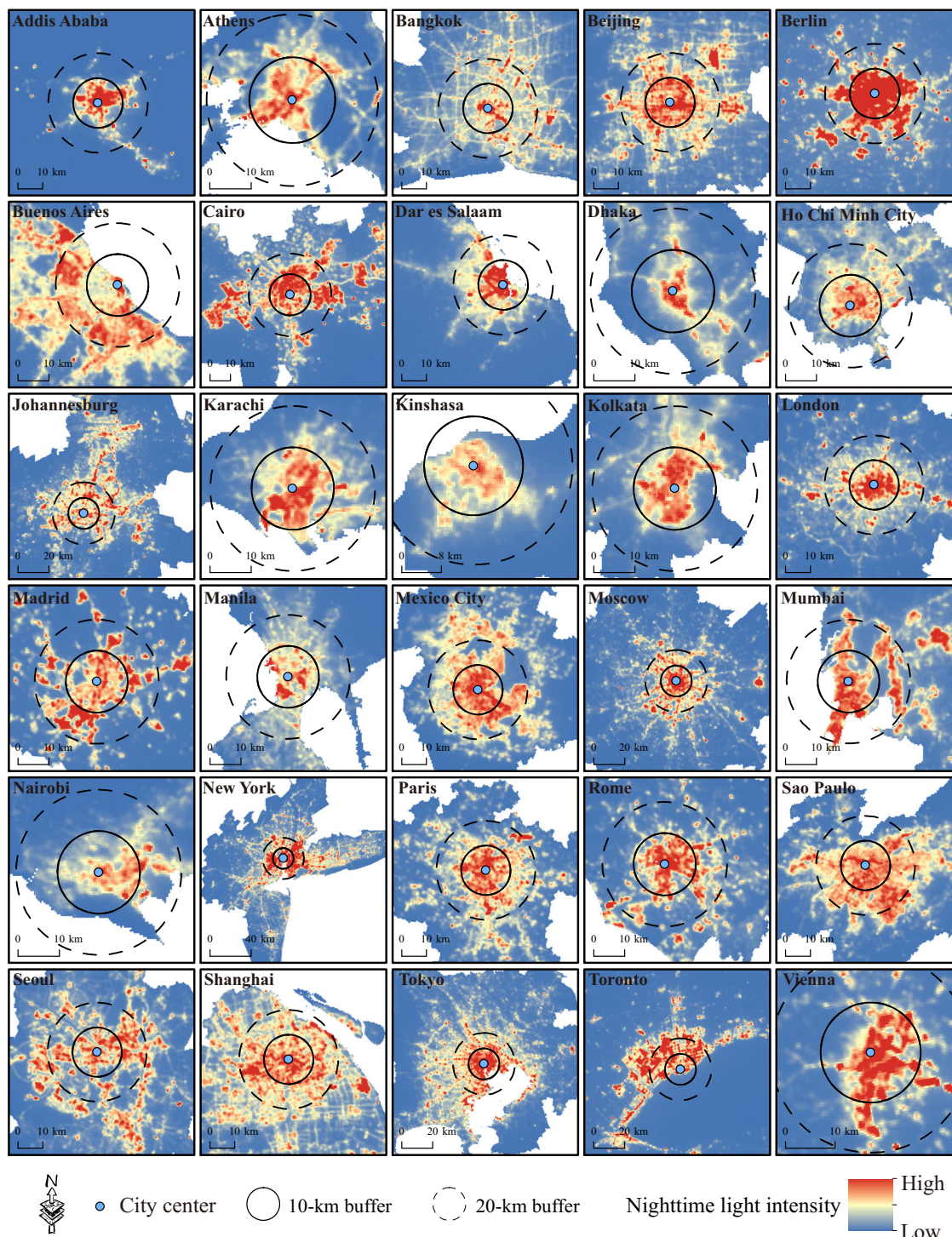
Fig. 4 Spatial distribution of nighttime light of 30 global megacities in 2020. Two buffers with radii of 10 km and 20 km show extents of sample cities. (Data Source: https://eogdata.mines.edu/nighttime_light/annual/v20/).

activities represented by nighttime light show stronger spatial agglomeration. The intensity of nighttime light is the highest in urban core areas and then decreases rapidly. In a fitting curve, the first decay interval is small, and the second decay interval accounts for a larger proportion, which means a more sprawling urban form in comparison. Except for Dhaka, Ho Chi Minh City, and Kolkata, the α values fitted by NLI of most cities are smaller than that of ULD. These cities are more compact in the physical space represented by urban land, while the urban form in the

social space symbolized by nighttime light is more sprawling (Fig. 6a). The values of parameter α of NLI in Dhaka, Ho Chi Minh City, and Kolkata are greater than that of ULD. The aggregation scope of NLI in these cities is smaller than urban entities. And these cities have more compact forms in social space, showing a more significant influence of city centers on socioeconomic activities.

The rapid expansion of megacities in physical space makes the density of urban land almost reach saturation. The population
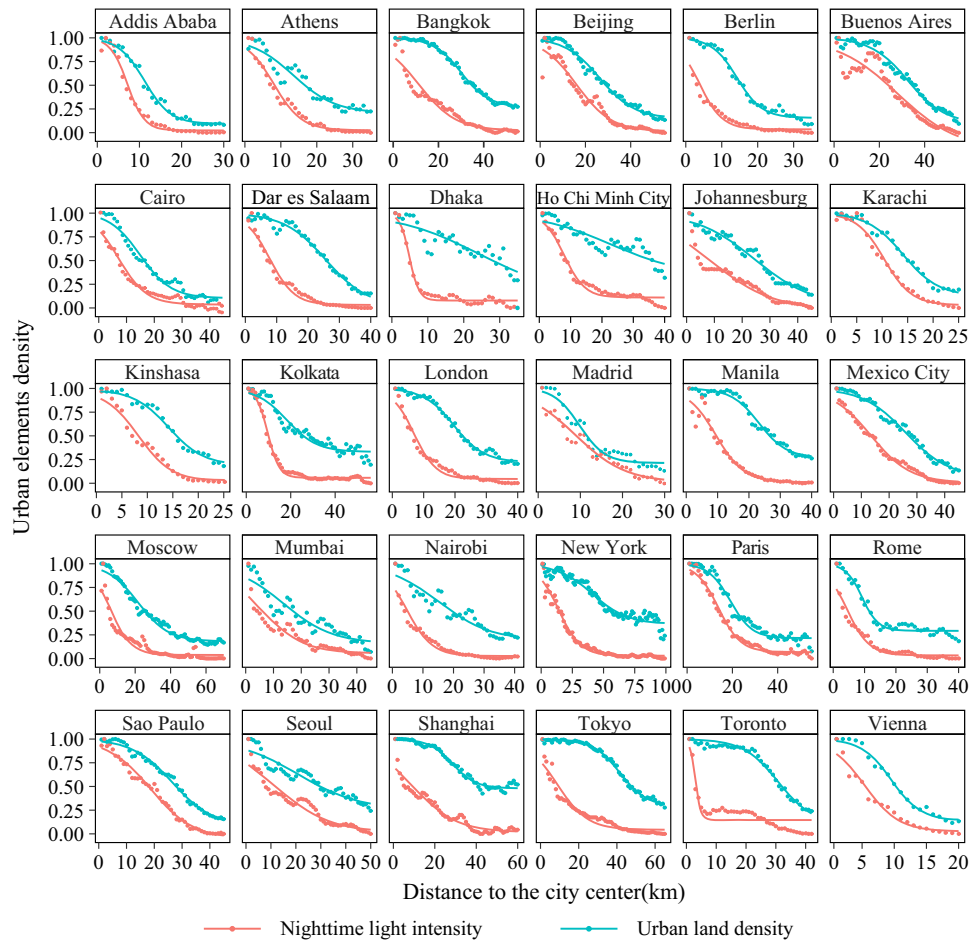
Fig. 5 Spatial gradients of urban land density and nighttime light intensity. ULD and NLI are calculated in a series of 1-km buffer rings with concentric ring analysis and NLI of each city has been normalized.

inside the cities is concentrated, and the gaps between urban centers and peripheries are too large. It results in an unbalanced population distribution, which is especially obvious in Tokyo and Shanghai. Similarly, this also causes the aggregation radii of NLI to be substantially smaller than the physical radii of the cities. In Fig. 5, the fitting curves of the two elements in Madrid are relatively similar, and the values of parameter D of Madrid are also relatively close. While in Fig. 6b, Tokyo, Shanghai, Toronto, New York, etc. with relatively large differences in fitted curves are mainly distributed in the upper left corner. The significant gap between the radii of nighttime light aggregation and urban entities highlights the disorderly expansion of cities and the consequent widening gap between physical and social space.

Cities are generally more or less sprawling and smaller in social space. Concentration degree index visualizes these differences across the cities in Fig. 7. The value of CDI is between 0.098 and 0.904, 0.474 on average. Toronto has the lowest value of CDI, but this does not mean that Toronto has a small urban radius in social space. As shown in Fig. 5, Toronto, Shanghai, Tokyo, and New York have very large urban entities, and NLI of these cities around city centers is so high that socioeconomic activities seem clustered only in the core area. As a result, these cities appear to have small radii in social space and urban forms that are not compact.

Urban structure of poly-centric cities. With the rapid urban expansion, many megacities have gradually developed an urban distribution pattern with a single main center and multiple sub-centers. For example, in Fig. 5 the scatter plots of urban elements

of Ho Chi Minh City and Seoul show slight fluctuations in the overall decay trend. These fluctuations are caused by the agglomeration of elements of other sub-centers. The Inverse-S function is also suitable for poly-centric cities by adjusting the buffer partitioning of cities (Jiao, 2015). Based on the fluctuations in the fitting curves, we chose Ho Chi Minh City and Seoul as poly-centric cities to adjust their buffer partitioning (Fig. 8).

According to the spatial distribution of nighttime light, other clustering places of nighttime light except for the CBD of cities can be determined. And the specific location of sub-centers of cities can be confirmed through the distance between the small and medium fluctuations of the fitting curves and the city centers. The buffer with the lowest density of urban land or the lowest intensity of nighttime light between the main center and a subcenter of a city is considered as the boundary of the area that the two centers can radiate. Figure 8 shows the spatial distribution of the main center and sub-centers of each city as well as their buffer partitioning.

From the parameters of fitting curves in Table 2, it demonstrates that the inverse-S function can be still applied to ULD and NLI well when using customized poly-centric buffers, and the fluctuations in fitting curves caused by sub-centers are significantly improved. By choosing proper city sub-centers and constructing reasonable poly-centric buffer zones, the inverse-S function can be applied to most cities, even if their spatial structure is varied. While it should be noted that spatial patterns of urban elements across different cities can be compared only with single-concentric buffers (Jiao, 2015).

Table 1 Parameters of inverse-S function for urban land density and nighttime light intensity.

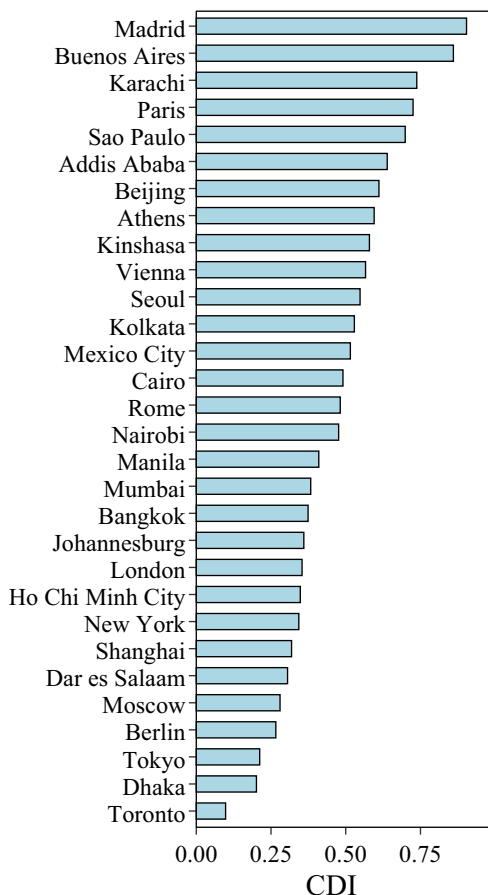| City	Urban land density				Nighttime light intensity			
	α	c	D	R^2	α	c	D	R^2
Addis Ababa, Ethiopia	3.64	0.09	22.42	0.988	3.56	0.02	14.32	0.984
Athens, Greece	2.31	0.21	27.11	0.914	2.09	0.02	16.13	0.996
Bangkok, Thailand	4.90	0.27	60.06	0.995	1.37	0.07	22.46	0.919
Beijing, China	3.43	0.15	52.57	0.984	2.08	0.01	32.12	0.955
Berlin, Germany	4.10	0.16	28.52	0.986	1.19	0.04	7.59	0.925
Buenos Aires, Argentina	4.03	0.10	65.32	0.962	2.10	0.06	56.18	0.896
Cairo, Egypt	2.74	0.14	30.63	0.969	1.49	0.08	15.03	0.954
Dar es Salaam, Tanzania	3.86	0.02	51.38	0.898	2.01	0.03	15.69	0.970
Dhaka, Bangladesh	2.14	0.14	48.65	0.929	3.67	0.08	9.79	0.975
Ho Chi Minh City, Vietnam	1.97	0.34	45.78	0.870	2.42	0.14	15.93	0.967
Johannesburg, South Africa	2.37	0.02	49.09	0.962	0.81	0.02	17.66	0.888
Karachi, Pakistan	4.06	0.13	28.20	0.987	3.86	0.05	20.80	0.987
Kinshasa, Republic of the Congo	4.19	0.17	28.49	0.984	2.57	0.01	16.50	0.975
Kolkata, India	2.71	0.33	36.67	0.936	3.73	0.06	19.39	0.990
London, UK	4.10	0.22	39.20	0.988	1.96	0.06	13.87	0.965
Madrid, Spain	3.25	0.21	19.79	0.954	1.49	0.01	17.89	0.942
Manila, Philippines	5.26	0.27	46.39	0.981	2.11	0.04	19.01	0.959
Mexico City, Mexico	3.38	0.06	52.21	0.983	1.89	0.03	26.91	0.984
Moscow, Russia	2.51	0.18	43.40	0.978	1.04	0.04	12.16	0.896
Mumbai, India	1.54	0.16	27.30	0.871	0.68	0.05	10.45	0.861
Nairobi, Kenya	1.72	0.38	18.88	0.992	1.21	0.04	8.99	0.995
New York, USA	2.92	0.37	81.74	0.941	1.58	0.04	28.04	0.869
Paris, France	3.98	0.22	38.24	0.935	2.82	0.07	27.73	0.976
Rome, Italy	3.55	0.29	18.4	0.966	1.25	0.04	8.86	0.931
Sao Paulo, Brazil	3.66	0.07	53.41	0.952	2.44	0.02	37.33	0.986
Seoul, Korea	1.71	0.26	41.87	0.891	1.04	0.03	22.94	0.916
Shanghai, China	5.05	0.48	57.00	0.981	0.86	0.09	18.17	0.992
Tokyo, Japan	5.92	0.29	83.00	0.995	1.11	0.04	17.61	0.932
Toronto, Canada	5.26	0.10	61.51	0.982	3.30	0.17	6.03	0.870
Vienna, Austria	4.15	0.14	19.04	0.988	2.03	0.05	10.78	0.963
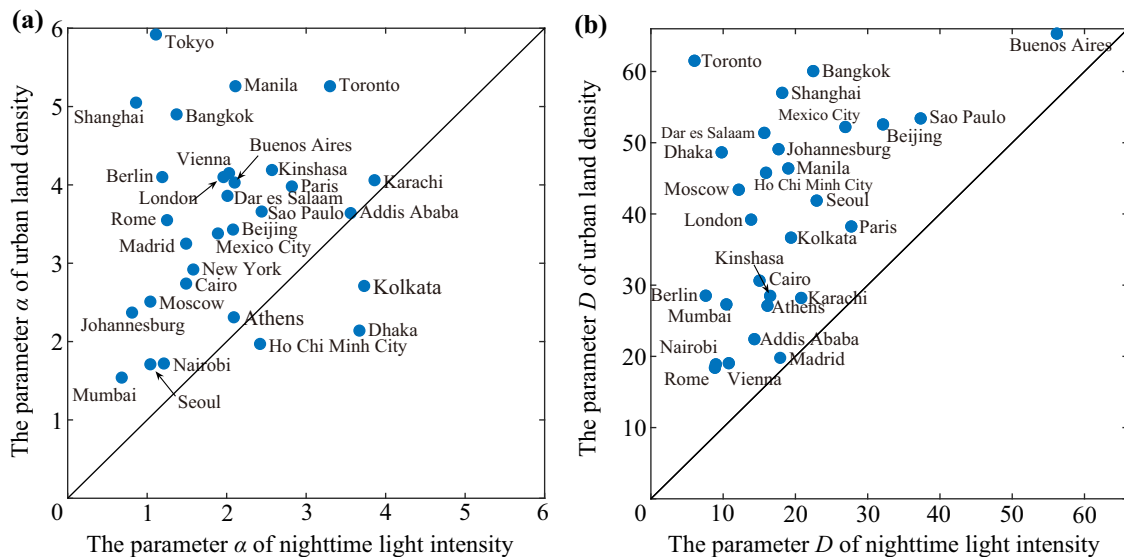
Fig. 6 Scatter plots of parameters of inverse-S function for urban land density and nighttime light intensity in concentric rings. a Parameter α. **b** Parameter D.

Discussion

In this study, we compare spatial gradients of urban land density and nighttime light intensity using the inverse-S function, which represents the physical and socioeconomic space of cities, respectively. Overall, both the urban land density and nighttime light intensity in concentric rings decrease with the distance to the city centers (Figs. 3 and 4). They first decrease slowly around city centers followed by a quick decay to suburban areas and then

Fig. 7 Concentration degree index (CDI) of 30 cities. The CDI is defined as the ratio of radii fitted by nighttime light intensity and urban land density.

decrease slowly again until the background level, showing an obvious inverse-S shape (Fig. 5). This spatial gradient can be well-fitted by the inverse-S function. This study first proves that the inverse-S function can also be applied to nighttime light intensity, which was originally proposed to characterize the spatial gradient of the urban land density.

Spatial agglomeration is a common characteristic of urban elements while urban land density and nighttime light intensity show different spatial gradients. The inverse-S function provides a more intuitive and reliable way of revealing the spatial distribution laws of different urban elements. Generally speaking, the parameters fitted by the inverse-S function of night light intensity and urban land density are quite different. The parameters α and D of NLI are both smaller than those of urban land density, and the aggregation radius of a city in social space is markedly smaller than the radius of the physical entity. From remote sensing images, some megacities also show high urban land density in the suburbs and urban fringes. As the areas within the cities are adjacent to each other, the urban form is more compact with the urban functions more complete (Bay, Lehmann, 2017). However, socioeconomic activities are more fragmented in the hinterland and more spatial agglomeration is shown.

Building inclusive, safe, resilient, and sustainable cities and communities is one of the United Nations' sustainable development goals (Fritz et al., 2019). A balanced relationship between urban expansion and population growth will promote sustainable urban development (Xu et al., 2019). For many

megacities with high populations, they are still expanding outwards and the upper limit of the population that they can accommodate is still rising (Angel et al., 2021). But the population density in urban core areas keeps high relatively and population distribution inside the cities may not match land use. It results in the increment of the cost and pressure of development in the central areas and the extravagance and waste caused by excessive expansion of the city boundary is also a major problem that needs to be solved urgently. Specific measures should be taken to enhance the coordinated and sustainable development of megacities in both physical and social spaces. The government needs to strengthen infrastructure construction in the suburbs and new urban areas to attract population migration from city centers and reduce the burden of resources in urban core areas (Xu et al., 2022).

In this study, nighttime light was used to represent the intensity of social and economic activities, and the density of urban land represented the actual development situation of cities. However, nighttime light cannot express the vitality of cities at daytime and urban land represents the level of development in two-dimensional space, ignoring the total available living space per unit area on a three-dimensional level. In further research, multi-source spatiotemporal data such as population density, road density, and urban three-dimensional building information can be added to understand and analyze the similarities and differences between physical and social space in the process of urbanization from multiple perspectives. In addition, temporal and spatial data can be used to conduct time series experiments to explore the distribution trends and relationships among various urban elements in the process of urban expansion.

Conclusion

This study uncovers different spatial patterns of the agglomeration of urban physical and socioeconomic elements. Taking 30 global megacities as examples, we use urban land and nighttime light to represent urban physical and social space, respectively. It is the spatial agglomeration of different types of urban elements that jointly determine the urban spatial structure and forms a complex urban system. Urban land density and nighttime light intensity share an overall trend of spatial gradients but with different details.

The urban land density function is also applicable for nighttime light intensity, and both urban land density and nighttime light intensity exhibit similar distribution patterns and "inverse-S" spatial gradients. The nighttime light intensity largely depends on the density of urban land. Higher density of built-up areas indicates greater nighttime light intensity, while the spatial gradient of the urban land density is flatter than that of nighttime light. In general, compared with the more fully developed urban land, the intensity of socioeconomic activities in megacities still has a large room for development. Areas of the cities in social space have a smaller coverage than those in physical space. The socioeconomic development of these megacities may not match the disorderly expansion of cities. How to mitigate or exploit this mismatch is worth paying attention to. The potential practical application of the proposed function is to compare the coordination of urban development in different spatial dimensions and to provide policy guidance for the sustainable development of megacities. In addition, the applicability of the inverse-S function can also be tested against other urban elements to explore a more complete mechanism of their spatial gradients.
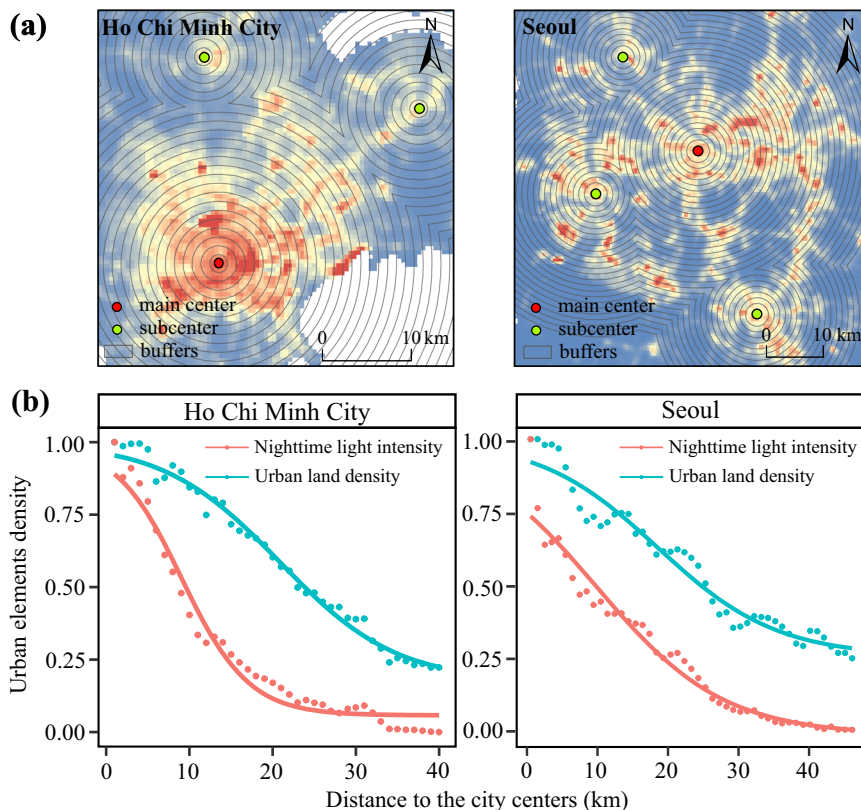
Fig. 8 Spatial gradients of urban land density and nighttime light intensity of poly-centric cities. a Buffer partitioning. **b** Spatial gradients.

Table 2 Parameters of inverse-S function for urban land density and nighttime light intensity of poly-centric cities.

City	Urban land density				Night-time light intensity			
	α	c	D	R^2	α	c	D	R^2
Ho Chi Minh City	2.98	0.17	41.69	0.986	2.27	0.06	18.20	0.974
Seoul	2.25	0.25	38.39	0.954	1.15	0.02	20.93	0.957

Data availability

Datasets used in this study are publicly accessed. Land use data was derived from ESRI 10-m global land-cover product (https://livingatlas.arcgis.com/landcover/). Nighttime light data was derived from the Earth Observation Group (https://eogdata.mines.edu/nighttime_light/annual/v20/).

References

Akbar TA, Hassan QK, Ishaq S et al. (2019) Investigative spatial distribution and modelling of existing and future urban land changes and its impact on urbanization and economy. Remote Sens 11(2):105

Angel S (2012) Planet of cities. Lincoln Institute of Land Policy, Cambridge, MA

Angel S, Lamson-Hall P, Blei A et al. (2021) Densify and expand: a global analysis of recent urban growth. Sustainability 13(7):3835

Bagan H, Yamagata Y (2012) Landsat analysis of urban growth: how Tokyo became the world's largest megacity during the last 40 years. Remote Sens Environ 127:210–222

Bagan H, Yamagata Y (2015) Analysis of urban growth and estimating population density using satellite images of nighttime lights and land-use and population data. GIsci Remote Sens 52(6):765–780

Batty M, Sik Kim K (1992) Form follows function: reformulating urban population density functions. Urban Stud 29(7):1043–1069

Bay JHP, Lehmann S (2017) Growing compact: urban form, density and sustainability. Taylor & Francis, London

Bennett MM, Smith LC (2017) Advances in using multitemporal night-time lights satellite imagery to detect, estimate, and monitor socioeconomic dynamics. Remote Sens Environ 192:176–197

Bonafoni S, Keeratikasikorn C (2018) Land surface temperature and urban density: Multiyear modeling and relationship analysis using MODIS and Landsat data. Remote Sens 10(9):1471

Burgess EW (2008) The growth of the city: an introduction to a research project. Springer, Boston, MA

Cai B, Shao Z, Fang S et al. (2021) Finer-scale spatiotemporal coupling coordination model between socioeconomic activity and eco-environment: a case study of Beijing, China. Ecol Indic 131:108165

Chen Y, Yang J, Yang R et al. (2022) Contribution of urban functional zones to the spatial distribution of urban thermal environment. Build Environ 216:109000

Christaller W (1966) Central places in southern Germany. Prentice-Hall, Englewood Cliffs, NJ

Duarte F, Álvarez R (2019) The data politics of the urban age. Palgrave Commun 5(1):1–7

Elvidge CD, Hsu FC, Zhizhin M et al. (2023) Statistical moments of VIIRS night-time lights. Int J Remote Sens:1–25. https://doi.org/10.1080/01431161.2022.2161857

Fritz S, See L, Carlson T et al. (2019) Citizen science and the United Nations sustainable development goals. Nat Sustain 2(10):922–930

Geddes P (1915) Cities in evolution: an introduction to the town planning movement and to the study of civics. Williams & Norgate, London

Govind NR, Ramesh H (2020) Exploring the relationship between LST and land cover of Bengaluru by concentric ring approach. Environ Monit Assess 192(10):1–25

Guérois M, Pumain D (2008) Built-up encroachment and the urban field: a comparison of forty European cities. Environ Plan A 40(9):2186–2203

Harris CD, Ullman EL (1945) The nature of cities. Ann Am Acad Polit Soc Sci 242(1):7–17

Huang X, Wen D, Li J et al. (2017) Multi-level monitoring of subtle urban changes for the megacities of China using high-resolution multi-view satellite imagery. Remote Sens Environ 196:56–75

Jiao L (2015) Urban land density function: a new method to characterize urban expansion. Landsc Urban Plan 139:26–39

Jiao L, Dong T, Xu G et al. (2021) Geographic micro-process model: understanding global urban expansion from a process-oriented view. Comput Environ Urban Syst 87:101603

Keeratikasikorn C (2018) A comparative study on four major cities in Northeastern Thailand using urban land density function. Geo Spat Inf Sci 21(2):93–101

Kroll F, Haase D (2010) Does demographic change affect land use patterns?: a case study from Germany. Land Use Policy 27(3):726–737

Kyba CC, Kuester T, Sánchez de Miguel A et al. (2017) Artificially lit surface of Earth at night increasing in radiance and extent. Sci Adv 3(11):e1701528

Letu H, Hara M, Yagi H et al. (2010) Estimating energy consumption from nighttime DMPS/OLS imagery after correcting for saturation effects. Int J Remote Sens 31(16):4443–4458

Levin N, Kyba CC, Zhang Q et al. (2020) Remote sensing of night lights: a review and an outlook for the future. Remote Sens Environ 237:111443

Li M, Verburg PH, van Vliet J (2022a) Global trends and local variations in land take per person. Landsc Urban Plan 218:104308

Li X-Y, Li X, Fan Z et al. (2022b) Civil war hinders crop production and threatens food security in Syria. Nat Food 3(1):38–46

Li X, Wang X, Zhang J et al. (2015) Allometric scaling, size distribution and pattern formation of natural cities. Palgrave Commun 1(1):1–11

Li Z, Jiao L, Zhang B et al. (2021) Understanding the pattern and mechanism of spatial concentration of urban land use, population and economic activities: a case study in Wuhan, China. Geo Spat Inf Sci 24(4):678–694

Mård J, Di Baldassarre G, Mazzoleni M (2018) Nighttime light data reveal how flood protection shapes human proximity to rivers. Sci Adv 4(8):eaar5779

McCallum I, Kyba CCM, Bayas JCL et al. (2022) Estimating global economic well-being with unlit settlements. Nat Commun 13(1):2459

Novotný J, Chakraborty S, Maity I (2022) Urban expansion of the 43 worlds' largest megacities: a search for unified macro-patterns. Habitat Int 129:102676

Patino JE, Duque JC (2013) A review of regional science applications of satellite remote sensing in urban settings. Comput Environ Urban Syst 37:1–17

Reba M, Seto KC (2020) A systematic review and assessment of algorithms to detect, characterize, and monitor urban land change. Remote Sens Environ 242:111739

Ren J, Yang J, Zhang Y et al. (2022) Exploring thermal comfort of urban buildings based on local climate zones. J Clean Prod 340:130744

Schneider A, Woodcock CE (2008) Compact, dispersed, fragmented, extensive? A comparison of urban growth in twenty-five global cities using remotely sensed data, pattern metrics and census information. Urban Stud 45(3):659–692

Scott AJ, Storper M (2015) The nature of cities: the scope and limits of urban theory. Int J Urban Reg Res 39(1):1–15

Seto KC, Fragkias M (2005) Quantifying spatiotemporal patterns of urban land-use change in four cities of China with time series landscape metrics. Landsc Ecol 20:871–888

Seto KC, Fragkias M, Güneralp B et al. (2011) A meta-analysis of global urban land expansion. PLoS ONE 6(8):e23777

Seto KC, Sánchez-Rodríguez R, Fragkias M (2010) The new geography of contemporary urbanization and the environment. Annu Rev Environ Resour 35(1):167–194

Shukla A, Jain K, Ramsankaran R et al. (2021) Understanding the macro-micro dynamics of urban densification: a case study of different sized Indian cities. Land Use Policy 107:105469

Song Z, Yu L (2019) Multifractal features of spatial variation in construction land in Beijing (1985–2015). Palgrave Commun 5(1):1–15

Taubenböck H, Wegmann M, Roth A et al. (2009) Urbanization in India–Spatiotemporal analysis using remote sensing data. Comput Environ Urban Syst 33(3):179–188

Van de Voorde T, Jacquet W, Canters F (2011) Mapping form and function in urban areas: an approach based on urban metrics and continuous impervious surface data. Landsc Urban Plan 102(3):143–155

Xiao R, Yu X, Xiang T et al. (2021) Exploring the coordination between physical space expansion and social space growth of China's urban agglomerations based on hierarchical analysis. Land Use Policy 109:105700

Xu G, Dong T, Cobbinah PB et al. (2019) Urban expansion and form changes across African cities with a global outlook: spatiotemporal analysis of urban land densities. J Clean Prod 224:802–810

Xu G, Su J, Xia C et al. (2022) Spatial mismatches between nighttime light intensity and building morphology in Shanghai, China. Sustain Cities Soc 81:103851

Xu G, Zhou Z, Jiao L et al. (2020) Compact urban form and expansion pattern slow down the decline in urban densities: a global perspective. Land Use Policy 94:104563

Yang J, Yuan M, Yang S et al. (2023) Spatial diffusion waves of human activities: evidence from harmonized nighttime light data during 1992–2018 in 234 cities of China. Remote Sens 15(5):1426

Yasin MY, Yusoff MM, Abdullah J et al. (2020) Is urban sprawl a threat to sustainable development? A review of characteristics and consequences. Geografia 16:4

Yu L, Zheng W, Yu T et al. (2021) How to identify urban centers/subcenters in metropolises? An analytical review. Habitat Int 115:102397

Zhang XQ (2016) The trends, promises and challenges of urbanisation in the world. Habitat Int 54:241–252

Acknowledgements

Author contributions

ZMC was responsible for the interpretation of the data and drafting of the work. HWL contributed to the conceptual framework and revision of the work. XG contributed to the conception and design of the work and revision of the work. LX was involved in the improvement of the design of the work. JLM made contributions to methodologies and revision of the work. All authors approved this version to be published and agreed to be accountable for all aspects of the work.

Competing interests

The authors declare no competing interests.

Ethics approval

This article does not contain any studies with human participants performed by any of the authors.

Informed consent

This article does not contain any studies with human participants performed by any of the authors.

Additional information

Correspondence and requests for materials should be addressed to Gang Xu.

Reprints and permission information is available at http://www.nature.com/reprints

Publisher's note Springer Nature remains neutral with regard to jurisdictional claims in published maps and institutional affiliations.